Advances in Nano Research, *Vol. 18, No. 1 (2025) 61-74*
https://doi.org/10.12989/anr.2025.18.1.061

Thermo-mechanical wave propagation in a viscous FG nanocomposite media based on the LS theory

Yi Yang[1a] and Chie Zhang*[2]

[1]*School of Civil Engineering Architecture and Environment, Hubei University of Technology, Wuhan 430000, Hubei, China*
[2]*School of Mechanical Engineering, Shanghai Jiao Tong University, Shanghai 200240, China*

(*Received November 18, 2021, Revised November 7, 2024, Accepted January 7, 2025*)

Abstract. The thermo-viscoelasticity of a functionally graded nano graphene platelet reinforced composite (FG-GPLRC) layer is investigated in the present examination. It is presumed that the nanoparticles are uniformly dispersed and arranged in random orientations within an arbitrary point of the one-dimensional domain. In addition, the distribution outline of the GPL volume fraction is based on a power-law model with a controller parameter. The second-order correlation homogenization method is employed to extract the equivalent thermomechanical characteristics of the under-study nanocomposite media. The viscous behavior of the structure is modeled by implementing the Kelvin-Voigt approach. Given that the structure experiences a sudden thermal shock, coupled thermoelasticity is utilized to obtain the governing equations. Moreover, the physical nature of the problem is modified by considering thermoelasticity in the generalized form following the Lord-Shulman (LS) model for the nanocomposite medium. To determine the response of the problem, the Generalized Differential Quadrature (GDQ) and Newmark approaches are applied. Unlike previous studies, which primarily focus on non-viscous or non-LS formulations, our research uniquely applies the LS model to address the thermo-mechanical wave propagation in a viscoelastic nanocomposite layer under thermal shock. This approach allows for more accurate modeling of the thermal responses in such advanced materials. After validating the demonstrated formulation and methods with available studies, multiple parametric cases are presented to thoroughly examine the response of the viscoelastic nanocomposite layer when subjected to rapid heating.
Keywords: FG-GPL nanocomposite reinforces layer; GDQ-Newmark Solution; generalized thermo-viscoelasticity; Lord-Shulman Theory

1. Introduction

In many industries where equipment and parts are in contact with heat, such as space structures or power plants, the applied heat rate is very high, and therefore calculations based on classical theories will be erroneous. For this reason, analysis of structures, especially new structures such as nanocomposites under rapid heating, seems to be essential. Under thermal loading, temperature in a structure behaves like a wave. The Fourier heat transfer laws lead to parabolic energy equations, suggesting instantaneous temperature propagation throughout the structure—an assumption that conflicts with the actual physical reality of the situation. Also, when the thermal loading is rapid or accompanied with a large amount, it is essential for the energy balance and dynamic equations to be fully integrated. In order to overcome these defects, within the domain of thermoelasticity, new coupled theories have been developed by considering the effect of the second sound (Hetnarski and Ignaczak 1999, 2000, Hetnarski and Eslami 2009). These theories depict temperature as being transmitted in the form of a wave that travels at a limited speed. Therefore, these models are called generalized thermoelasticity theories. On the other hand, layers are non-curved environments that are considered one-dimensional or two-dimensional as well as bounded or unbounded and have many applications in various industries. Among the most prominent generalized theories is the Lord-Shulman (LS) theory. By taking into account a relaxation time and the rate of heat flux, this theory transforms the energy balance equation from a parabolic to a hyperbolic form (Lord and Shulman 1967). Other common theories scrutinized by researchers include Green-Naghdi (Green and Naghdi 1991, 1992), Green-Lindsay (Green and Lindsay 1992), and phase-lag (Tzou 1995).

1.1 Background

The effect of thermal shock on isotropic layers based on coupling and generalized theories has been widely studied in the mechanical literature. Kiani and Eslami (2017) investigated the LS-based linear coupled thermoelastic response of an isotropic layer utilizing generalized differential quadrature method. They also used Picard iterative technique to solve the non-linear energy equation. Taheri *et al*. (2004) studied the thermal and mechanical behavior of 1D finite domain made of homogeneous and isotropic materials and formulated by considering the Green-Naghdi theory. Zad *et al*. (2012) proposed the unified model of coupled and uncoupled generalized theories, counting the theory of LS, Green-Naghdi, and Green-

*Corresponding author, Ph.D.,
E-mail: chie.zhang.sjtu@gmail.com
[a] Ph.D., Email: yangyi980915@163.com

ISSN: 2287-237X (Print), 2287-2388 (Online)

Lindsey, to investigate the effect of thermal loading on a one-dimensional domain of a finite length. In their research, finite element method (FEM) is implemented to obtain the reaction of layer. This problem also solved by Bagri *et al*. (2006a) utilizing a closed form solution technique. The identical unified representation for the semi-infinite 1D medium subjected to laser wave packet has been examined by Youssef and El-Bary (2014). On the other hand, Wang *et al*. (2012) introduced a unified formulation of thermo-elasticity based on the dependent on temperature rate, extended, and not based on assumptions regarding energy dissipation. Yu *et al*. (2014) proposed the thermoelastic response that depends on time for a flat layer with length L. This issue is grounded in the revised LS theory refined by applying the Kernel function. Youssef and Al-Lehaibi (2007) proposed a state space formulation for obtaining the two-temperature generalized thermoelasticity of a unlimited strip. Youssef and Alghamdi (2020) introduced a generalized format of dual-phase-lags concept intended for the swift heating of epidermal tissue. Laplace transformation and Tzuo procedures are employed to attain the problem response. Alihemmati *et al*. (2021) applied the Chebyshev collocation tool to solve the unified generalized problem of a bounded strip. Hosseini-Tehrani and Eslami (2000a, b, 2003) prosperously employed boundary element procedure to examine the linear generalized thermoelasticity of a flat and rectangular environment. Youssef (2006) figured the thermoelastic wave propagation of a 2D half-space materials based on the LS concept. He employed Fourier and Laplace transformation to calculate the feedback. An analysis is conducted on coupled generalized heating shock in a two-dimensional half-space system utilizing the Green-Naghdi second sound scheme by Othman *et al*. (2009).

Misra and Samanta (1982) analyzed the influence of considering thermal relaxation on the viscoelastic wave propagation under rapid heating of a half-space domain. Othman (2005) introduced a type of generalized thermo-viscoelasticity formulation under various thermal loading at a half-space environment. The normal mode analysis was implemented to extract the unknown variables of this problem. Moreover, the rotation impacts with on relaxation time is considered. A thermal stress analysis is performed to understand the behavior of an infinite viscous region by Kartashov (2014). Two various rheological model is employed namely: Maxwell and Kelvin. Ezzat *et al*. (2002) established the thermo-viscoelasticity of two-dimensional media with one relaxation time. Pobedria and Fung's model of rheological formulations is selected to perform this study. Fourier and Laplace transformation is exploited to solve this problem. Roychoudhuri and Mukhopadhyay (2000) combined the two Green-Lindsay model for the thermo-elasticity part and the Kelvin-Voight model for the viscosity part. Then, they applied the resulting formulation to an infinite boundless environment to investigate the response of this medium to thermal shock. Within the framework of Green-Naghdi theories of type II and III and also three-phase-lag model, Kanoria and Mallik (2010) proposed a formulation to obtain the response of an infinite media under the periodically varying heat sources. The effect of applied voids in a one dimensional viscoelastic media on the thermally behavior is examined by Sharma and Kumar (2013). Three longitudinal waves, elastic, thermal, and volume fraction, were observed to propagate in a porous medium. Rakshit and Mukhopadhyay (2007) offered a linear integral form for constitutive law of 2D media exposed to instantaneous point heat source. They solved this problem utilizing eigenvalue procedure. Mirzaei (2020) investigated the thermally nonlinear thermoviscoelasticity of an isotropic strip under thermal shock. In this paper the thermomechanical wave propagation in the finite domain is examined. This research is also solved by Oskouie *et al*. (2020) utilizing the variational differential quadrature method.

Karimi Zeverdejani and Kiani (2020) implemented a hybrid GDQ-Newmark-Picard technique to verify the Lord-Shulman-based generalized thermoelasticity of FG layers. It is considered that the material properties changes based on an exponential function. Bagri *et al*. (2006b) studied the thermoelastic behavior of FG layers under the Lord-Shulman assumption. Galerkin-based finite element and Laplace technique is utilized to extract the layer response. Nikolarakis and Theotokoglou (2017) developed the generalized unified formulation of thermoelasticity based on the Lord-Shulman, Green-Naghdi, and Green-Lindsay to study the rapid heating of three layered functionally graded strips. Hashemi *et al*. (2021a) investigated the thermally induced instability of CNTRC panels under functionally graded nanoparticle distributions.

Nanocomposites have emerged as revolutionary materials in mechanical and thermal applications (Zhang *et al*. 2015, Yang *et al*. 2017a, Gao *et al*. 2019). offering enhanced strength, durability, and heat resistance due to their unique nanoscale reinforcement, which allows for superior performance in demanding environments and critical industries (Gao *et al*. 2020). For example, in lubricant conditions (Yang *et al*. 2019) and nanofluid (Yang *et al*. 2020), this materials with FG distributions can act with high performance. Graphene or graphene platelet (GPL) reinforcement is among the most commonly utilized forms of nanocomposites. Thin-walled structures composed of these materials have been extensively analyzed in contexts such as free and forced vibration (Xu *et al*. 2021, Habibi *et al*. 2019a, Arefi *et al*. 2018, Hashemi *et al*. 2021b, Oyarhossein *et al*. 2020) stability (Chen *et al*. 2022, Hajilak *et al*. 2019), bending (Arefi *et al*. 2019a, 2020), thermal static response (Arefi *et al*. 2019b, Arefi 2019c), and mechanical wave propagation (Ebrahimi *et al*. 2019, Habibi *et al*. 2019b, Moradi *et al*. 2024) behaviors. Another application of nanocomposite materials is energy absorption in various devices (Shao *et al*. 2021, Guo *et al*. 2021b).

1.2 Voids in the literature

Reviewing the literature on thermo-mechanical problems, we find that only several scientific papers on the generalized thermoelasticity of GPL-reinforced nano-composite structures have been introduced. Hosseini and Zhang (2018) proposed rapid heating formulation of FG-GPLRC cylinders considering the generalized thermo-elasticity based on the Green-Naghdi with energy

dissipation. This problem is solved by a meshless technique based on the generalized finite difference method. Afterward, Heydarpour *et al*. (2019, 2020) investigated the coupled tharmoelastic response of hollow spheres and cones implementing the layer-wise differential quadrature method in the structure field. In addition, a time integrating scheme based on the non-uniform rotational B-spline linkage with Newmark are utilized to solve the ordinary differential equations in the time domain. Unlike previous studies, which primarily focus on non-viscous or non-LS formulations, our research uniquely applies the LS model to address the thermo-mechanical wave propagation in a viscoelastic nanocomposite layer under thermal shock. This approach allows for more accurate modeling of the thermal responses in such advanced materials. The proposed method has significant potential in fields where advanced thermal management is crucial, such as aerospace, electronics, and nanotechnology. Specifically, understanding the thermo-mechanical behavior of functionally graded graphene platelet reinforced composites (FG-GPLRCs) under thermal shock can be valuable for designing materials that endure extreme thermal environments, such as high-speed aircraft surfaces, thermal barriers, and high-power electronic components. By implementing the Lord-Shulman theory in analyzing thermal shock effects, this study offers a more accurate model for predicting how viscoelastic nano-composite materials respond to sudden thermal changes. This insight is essential for enhancing material durability and performance in environments requiring precise control over temperature-induced stresses. Therefore, in the current study, the effect of heat shock on viscoelastic nano-composite layers based on Lord-Shulman theory, which is one of the second sound modifier theories, is investigated. The GPLs distribution applied in the one-dimensional domain is assumed based on a power law function. The GDQ and Newmark methods are successfully applied in this problem to extract the thermoelastic wave propagation in the finite strip. The effect of viscosity factor, relaxation time, GPL weight fraction and its functionally grading on the thermoelastic behavior of the layer is scrutinized.

2. FG-GPLRC finite domain

In the present study, a one-dimensional viscous domain reinforced with functionally graded nano graphene platelets is considered. This layer with finite length L is subjected to thermal shock at its edge (Fig. 1).

The variation of nano particle volume fraction is in the direction of the layer length and is based on the power law function as

$$V_{GPL}(x) = (1 - \frac{x}{L})^{\zeta} V^{\star}_{GPL} \tag{1}$$

where ζ defines how GPLs are distributed throughout the layer and assumes only zero and positive amounts. Except when this value is zero, the amount of GPL at the end of the layer is zero. When the power law index is zero, the entire nanocomposite layer will have constant GPL volume fraction $V^{\star}_{GPL}$. Therefore, increasing the power law index reduces the total volume fraction of GPL in the layer. It

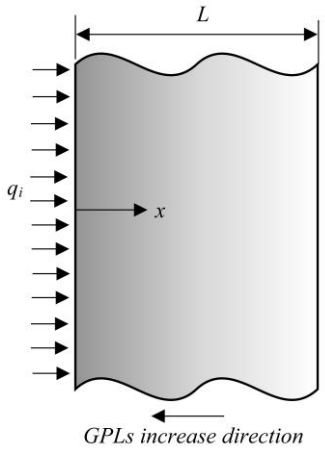

Fig. 1 View of an FG-GPLRC layer under thermal shock

should be noted that $V^{\star}_{GPL}$ represents the most GPL applied to the beginning of the layer $x = 0$. This amount can be computed in terms of the GPL weight fraction W_{GPL}, GPL mass density ρ_{GPL}, and matrix mass density ρ_m as

$$V^{\star}_{GPL} = \frac{W_{GPL}}{W_{GPL} + \left(\frac{\rho_{GPL}}{\rho_m}\right)(1 - W_{GPL})} \tag{2}$$

Throughout this paper, m index is related to the matrix constituent and the GPL index is related to GPL particles. The effective elasticity modulus E of each arbitrary point of the layer is determined utilizing the Halpin-Tsai micro-mechanical rule (Affdl and Kardos 1976, Dong *et al*. 2022). This rule can be expressed by

$$E(x) = \frac{3}{8}\frac{1 + \xi_L \eta_L V_{GPL}}{1 - \eta_L V_{GPL}} E_m + \frac{5}{8}\frac{1 + \xi_T \eta_T V_{GPL}}{1 - \eta_T V_{GPL}} E_m \tag{3}$$

This rule is a second-order correlation homogenization method that also considers the effects of the size and shape of the reinforcing particles in obtaining the equivalent property. η_L and η_T are two parameters determined by

$$\eta_L = \frac{\left(\frac{E_{GPL}}{E_m}\right) - 1}{\left(\frac{E_{GPL}}{E_m}\right) + \xi_L}, \quad \eta_T = \frac{\left(\frac{E_{GPL}}{E_m}\right) - 1}{\left(\frac{E_{GPL}}{E_m}\right) + \xi_T} \tag{4}$$

where geometric ratios in these parameters are defined as follows

$$\xi_L = 2\left(\frac{a_{GPL}}{t_{GPL}}\right), \quad \xi_T = 2\left(\frac{b_{GPL}}{t_{GPL}}\right) \tag{5}$$

To derive the effective thermal conductivity k of the nanocomposite, the interaction direct derivative (IDD) model, which is an explicit scheme derived from the effective self-consistent scheme (ESCS) technique, is employed (Zheng and Du 2001, Chu *et al*. 2012). In addition, this analytical model is a second-order homogenization rule that applies the effects of particle size and shape used in the matrix. Based on this model we have

$$k(x) = k_m \left\{1 + \frac{V_{GPL}}{3}\left[\frac{2}{H + 1/(k_x/k_m - 1)} + \frac{1}{(1 - H)/2 + 1/(k_z/k_m - 1)}\right]\right\} \tag{6}$$

The aspect ratio-dependent parameter H can be calculated by

$$H(\xi_L)=\frac{\ln(\xi_L/2+\sqrt{(\xi_L/2)^2-1})(\xi_L/2)}{\sqrt{((\xi_L/2)^2-1)^2}}-\frac{1}{(\xi_L/2)^2-1} \quad (7)$$

Due to the thermal barrier between GPL and the matrix, the interfacial thermal resistance coefficient R_k is defined. This coefficient acts as a coating on the GPL surfaces and reduces the thermal conductivity of the graphene k_{GPL}.

$$k_x=\frac{k_{GPL}}{2R_k h_{GPL}/a_{GPL}+1}, \qquad k_z=\frac{k_{GPL}}{2R_k h_{GPL}/t_{GPL}+1} \quad (8)$$

where k_x and k_z indicate the equivalent thermal conductivity of GPL along its length and thickness, respectively. The effective state of the other thermo-mechanical properties is obtained using Voigt's law due to the small difference between the magnitudes of matrix and the GPL (Esmaeilzadeh *et al*. 2021, Safari *et al*. 2021).

$$\begin{aligned}\rho(x)&=\rho_{GPL}V_{GPL}+\rho_m(1-V_{GPL})\\ c(x)&=c_{GPL}V_{GPL}+c_m(1-V_{GPL})\\ \alpha(x)&=\alpha_{GPL}V_{GPL}+\alpha_m(1-V_{GPL})\end{aligned} \quad (9)$$

in which ρ, c, and α demonstrate the effective mass density, specific heat capacity, and thermal expansion within the layer, respectively. It should be noted that the viscosity factor τ and the thermal relaxation time t_0 are assumed to be constant along the domain.

3. Motion equation

The most general state of linear viscosity can be expressed in the form of integral equations in the style of the Volterra equation (Javani *et al*. 2021)

$$\varepsilon^m=\int_0^t \dot{D}(t-\chi)\sigma\, d\chi \quad (10)$$

where ε^m and σ denote the mechanical strain and stress tensors. Besides, a dot over a variable concludes the time differentiation. D is called the creep function. Kelvin-Voight model, the most widely employed model for viscous structures, well examines the creep behavior of the structure. This model estimates the creep function as follows

$$D(t)=C^{-1}(1-\exp(-t/\tau)) \quad (11)$$

in which C is the elasticity constant tensor. Moreover, τ indicates the viscosity factor which is assumed constant in the whole layer. The Kelvin-Voigt model implements the viscosity characteristic by modeling the spring and damper in parallel. Substituting Eq. (11) into Eq. (10), and considering only one-dimensional type of stress-strain relations, it can be written that

$$\sigma_{xx}=E\left(1+\tau\frac{\partial}{\partial t}\right)(\varepsilon_{xx}-\varepsilon_{xx}^T) \quad (12)$$

In the above equation the mechanical strain ε_{xx}^m is replaced by $\varepsilon_{xx}-\varepsilon_{xx}^T$ which ε_{xx} and ε_{xx}^T illustrate in order the total and thermal strains. This equation can be used for plane stress layer. Therefore, the thermal strain can be defined $\varepsilon_{xx}^T=\alpha(T-T_0)$. Furthermore, T and T_0 are the temperature along the layer and reference temperature, respectively.

The motion equation in one-dimensional domain in the absence of body forces can be taken the following form

$$\sigma_{xx,x}=\rho\ddot{u} \quad (13)$$

where u is axial displacement and its relation with the total strain for the infinitesimal theory, may be represented by

$$\varepsilon_{xx}=u_{,x} \quad (14)$$

Placing the Eq. (14) in Eq. (12) and then placing the result in the equation of motion, this equation can be expressed as a function of displacement and temperature as follows

$$\begin{aligned}Eu_{,xx}+E_{,x}u_{,x}-\beta T_{,x}-\beta_{,x}(T-T_0)+\tau E\dot{u}_{,xx}\\ +\tau E_{,x}\dot{u}_{,x}-\tau\beta\dot{T}_{,x}-\tau\beta_{,x}\dot{T}-\rho\ddot{u}=0\end{aligned} \quad (15)$$

where β is the thermoelastic parameter described by $\beta=E\alpha$. In order to complete the equations of motion, it is necessary to define boundary conditions. The mechanical boundary conditions of the present problem are defined as follows

$$\begin{aligned}x=0:&\quad u=0\\ x=L:&\quad \sigma_{xx}=0\end{aligned} \quad (16)$$

4. Energy equation

As is well known, the energy equation based on the definition of heat according to the Fourier law has infinite wave velocity due to its parabolic nature. This definition contradicts reality because temperature, like displacement and stress, travels as a wave at a finite speed. Various ideas have been proposed to generalize this concept in order to correct it. One of the most widely exploited theories is the Lord-Shulman theory, which attempts to correct the Fourier law by considering the relaxation time in the definition of the heat equation. This theory is expressed as follows (Hetnarski and Eslami 2009)

$$q+t0q=-kT,x \quad (17)$$

in which q depicts the heat flux and t_0 exhibits the relaxation time which is assumed to be constant as mentioned earlier. The energy equation related to the thermally linear theory, can be extracted utilizing the second law of thermodynamic as

$$-q_{,x}=T_0\dot{S} \quad (18)$$

S is the structure entropy which depends on the strain and temperature. Therefore, the derivative of this variable with respect to t can be attained implicitly as follows

$$\dot{S}=\frac{\partial S}{\partial\varepsilon_{xx}}\dot{\varepsilon}_{xx}+\frac{\partial S}{\partial T}\dot{T} \quad (19)$$

The above relation can be written more simply by

defining the free energy and the Gibbs energy, but for the sake of brevity only the final form is given here and reader can refer to Hetnarski and Eslami (2009) for more details.

$$T_0\dot{S} = T_0\beta\dot{\varepsilon}_{xx} + \rho c\dot{T} \tag{20}$$

Although the energy equation in this paper is considered completely coupled, by ignoring the first term of the above equation, the uncoupled thermoelasticity equations can be extracted. Implementing Eq. (14), (17), (18), and (20), the equation of energy can be denoted in terms of displacement and temperature.

$$kT_{,xx} + k_{,x}T_{,x} - T_0\beta\dot{u}_{,x} - t_0T_0\beta\ddot{u}_{,x} - \rho c\dot{T} - t_0\rho c\ddot{T} = 0 \tag{21}$$

The boundary conditions of the energy equation for this problem are defined as follows

$$\begin{aligned} x = 0: &\quad -kT_{,x} = q_i \\ x = L: &\quad T = T_0 \end{aligned} \tag{22}$$

5. Dimensionless equations

In order to better investigate the thermomechanical properties of the layer, the equations of motion and energy can be solved in dimensionless form applying the following non-dimensional parameters.

$$\begin{aligned} &\bar{x} = \frac{x}{l}, \quad \bar{L} = \frac{L}{l}, \quad (\bar{t}, \bar{t}_0, \bar{\tau}) = (t, t_0, \tau)\frac{C_{em}}{l}, \\ &\bar{\sigma}_{xx} = \frac{\sigma_{xx}}{E_m\alpha_m T_0}, \qquad \bar{u} = \frac{u}{\alpha_m T_0 l}, \\ &\bar{\theta} = \frac{T - T_0}{T_0}, \quad \bar{q} = \frac{ql}{k_m T_0} \end{aligned} \tag{23}$$

where the symbol $(\bar{})$ indicates that the variable is dimensionless. Factor l is a characteristic length defined as

$$l = \frac{\eta_m}{C_{em}} \tag{24}$$

Here, η_m and C_{em} are thermal diffusivity and speed of displacement wave propagation in the pure matrix media which are described by

$$\eta_m = \frac{k_m}{\rho_m c_m}, \qquad C_{em} = \sqrt{\frac{E_m}{\rho_m}} \tag{25}$$

With the aid of the parameters defined in Eq. (23), the equations of motion and energy that are completely coupled can be written below in dimensionless form.

$$\begin{aligned} &\bar{E}\bar{u}_{\bar{x}\bar{x}} + \bar{E}_{,\bar{x}}\bar{u}_{,\bar{x}} - \bar{\beta}\bar{\theta}_{,\bar{x}} - \bar{\beta}_{,\bar{x}}\bar{\theta} + \bar{\tau}\bar{E}\dot{\bar{u}}_{\bar{x}\bar{x}} + \bar{\tau}\bar{E}_{,\bar{x}}\dot{\bar{u}}_{,\bar{x}} \\ &\quad -\bar{\tau}\bar{\beta}\dot{\bar{\theta}}_{,\bar{x}} - \bar{\tau}\bar{\beta}_{,\bar{x}}\dot{\bar{\theta}} - \bar{\rho}\ddot{\bar{u}} = 0 \\ &\bar{k}\bar{\theta}_{,\bar{x}\bar{x}} + \bar{k}_{,\bar{x}}\bar{\theta}_{,\bar{x}} - C_T\bar{\beta}\dot{\bar{u}}_{,\bar{x}} - \bar{t}_0C_T\bar{\beta}\ddot{\bar{u}}_{,\bar{x}} \\ &-\bar{\rho}\bar{c}\dot{\bar{\theta}} - \bar{t}_0\bar{\rho}\bar{c}\ddot{\bar{\theta}} = 0 \end{aligned} \tag{26}$$

The material properties used in the above equations can be derived in the following representation

$$\bar{E} = \frac{E}{E_m}, \quad \bar{\beta} = \frac{E\alpha}{E_m\alpha_m}, \quad \bar{\rho} = \frac{\rho}{\rho_m}, \tag{27}$$

$$\bar{k} = \frac{k}{k_m}, \quad \bar{c} = \frac{c}{c_m}$$

Moreover, C_T is coupling coefficient which is specified by the following relation

$$C_T = \frac{T_0E_m\alpha_m^2}{\rho_m c_m} \tag{28}$$

In the continuation of the article, all the equations are stated dimensionless and in order to observe the brevity and simplicity, the symbol $(\bar{})$ has been removed from the variables.

6. Solution procedure

First it is need to derive the equations of motion and energy algebraically. This process has been performed implementing the generalized differential quadrature approach in this research. This method, which is well documented in the discussion of equations solving, is a significant practical and simple tool for extracting equations in algebraic form. Details of the solution method are not given here, but everyone can refer to Kiani and Eslami (2017), Guo *et al*. (2021a). After applying this method Eq. (26) takes the following matrix form

$$\begin{aligned} &\begin{bmatrix} [M^{uu}] & [M^{u\theta}] \\ [M^{\theta u}] & [M^{\theta\theta}] \end{bmatrix}\begin{Bmatrix} \{\ddot{u}\} \\ \{\ddot{\theta}\} \end{Bmatrix} + \begin{bmatrix} [C^{uu}] & [C^{u\theta}] \\ [C^{\theta u}] & [C^{\theta\theta}] \end{bmatrix}\begin{Bmatrix} \{\dot{u}\} \\ \{\dot{\theta}\} \end{Bmatrix} \\ &\quad + \begin{bmatrix} [K^{uu}] & [K^{u\theta}] \\ [K^{\theta u}] & [K^{\theta\theta}] \end{bmatrix}\begin{Bmatrix} \{u\} \\ \{\theta\} \end{Bmatrix} = \begin{Bmatrix} \{F^u\} \\ \{F^\theta\} \end{Bmatrix} \end{aligned} \tag{29}$$

where each component of the parts of mass, damping, and stiffness matrices associate with the parts of the force vector can be acquired from the following relations

$$\begin{aligned} M_{ij}^{uu} &= -\rho_i C_{ij}^{(0)} \\ M_{ij}^{u\theta} &= 0 \\ M_{ij}^{\theta u} &= -t_0 C_T \beta_i C_{ij}^{(1)} \\ M_{ij}^{\theta\theta} &= -t_0 \rho_i c_i C_{ij}^{(0)} \\ C_{ij}^{uu} &= \tau E_i C_{ij}^{(2)} + \tau E_{i,x} C_{ij}^{(1)} \\ C_{ij}^{u\theta} &= -\tau\beta_i C_{ij}^{(1)} - \tau\beta_{i,x} C_{ij}^{(0)} \\ C_{ij}^{\theta u} &= -C_T\beta_i C_{ij}^{(1)} \\ C_{ij}^{\theta\theta} &= -\rho_i c_i C_{ij}^{(0)} \\ K_{ij}^{uu} &= E_i C_{ij}^{(2)} + E_{i,x} C_{ij}^{(1)} \\ K_{ij}^{u\theta} &= -\beta_i C_{ij}^{(1)} - \beta_{i,x} C_{ij}^{(0)} \\ K_{ij}^{\theta u} &= 0 \\ K_{ij}^{\theta\theta} &= k_i C_{ij}^{(2)} + k_{i,x} C_{ij}^{(1)} \\ F_i^u &= 0 \end{aligned} \tag{30}$$

$$F_i^{\theta}=0,\quad i=2,\dots,N_x-1, j=1,2,\dots,N_x$$

where in the first and last lines of parts of matrices, the boundary conditions must be satisfied. So, we have

$$\begin{gathered}
M_{1j}^{uu}=0,\quad M_{1j}^{u\theta}=0,\quad M_{1j}^{\theta u}=0,\quad M_{1j}^{\theta\theta}=0\\
M_{N_xj}^{uu}=0,\quad M_{N_xj}^{u\theta}=0,\quad M_{N_xj}^{\theta u}=0,\quad M_{N_xj}^{\theta\theta}=0\\
C_{1j}^{uu}=0,\quad C_{1j}^{u\theta}=0,\quad C_{1j}^{\theta u}=0,\quad C_{1j}^{\theta\theta}=0\\
C_{N_xj}^{uu}=\tau E_{N_x}C_{N_xj}^{(1)},\quad C_{N_xj}^{u\theta}=-\tau\beta_{N_x}C_{N_xj}^{(0)},\quad C_{N_xj}^{\theta u}=0,\quad C_{N_xj}^{\theta\theta}=0\\
K_{1j}^{uu}=C_{1j}^{(0)},\quad K_{1j}^{u\theta}=0,\quad K_{1j}^{\theta u}=0,\quad K_{1j}^{\theta\theta}=-k_1C_{1j}^{(1)}\\
K_{N_xj}^{uu}=E_{N_x}C_{N_xj}^{(1)},\quad K_{N_xj}^{u\theta}=-\beta_{N_x}C_{N_xj}^{(0)},\quad K_{N_xj}^{\theta u}=0,\quad K_{N_xj}^{\theta\theta}=C_{N_xj}^{(0)}\\
F_1^{u}=0,\quad F_1^{\theta}=q_i,\quad F_{N_x}^{u}=0,\quad F_{N_x}^{\theta}=0
\end{gathered}\tag{31}$$

In the above equations $C_{ij}^{(0)}$, $C_{ij}^{(1)}$, and $C_{ij}^{(2)}$ are the weighting coefficients related to the zero-, first-, and second-order derivatives. Also, N_x is the number of distributed nodes along the domain. Each of non-dimensional displacement and temperature vectors contains N_x components as $\{u\}=\{u_1,u_2,..,u_i,\dots u_{N_x}\}^T$ and $\{\theta\}=\{\theta_1,\theta_2,..,\theta_i,\dots\theta_{N_x}\}^T$. It is worth noting that u_i is the dimensionless displacement of node i. The well-known Gauss-Lobatto-Chebyshev type of nodal distribution models is employed to discrete the layer dimensionless domain $0\le x\le L$. one can be written

$$x_i=L\left(\frac{1}{2}-\frac{1}{2}\cos\left(\frac{p-1}{N_x-1}\pi\right)\right),\qquad i=1,2,\dots,N_x \tag{32}$$

After applying the boundary conditions to the discrete equations, the Newmark time marching procedure has been executed in order to solve the equations in the time domain. The Newmark procedure used in this article is based on the constant average acceleration technique ($\alpha'=0.5,\beta'=0.25$) (Javani *et al*. 2019, Akbas 2018, Ebrahimi and Habibi 2017). After applying the Newmark method, the equations are obtained as follows

$$\hat{\mathbf{K}}\mathbf{X}_{s+1}=\hat{\mathbf{F}}_{s,s+1} \tag{33}$$

where $\hat{\mathbf{K}}$ and $\hat{\mathbf{F}}_{s,s+1}$ are the generalized stiffness matrix and the generalized force vector related to the time $t=(s+1)\Delta t$ and they can be written

$$\begin{gathered}
\hat{\mathbf{K}}_{s+1}=\mathbf{K}_{s+1}+\frac{1}{\beta'\Delta t^2}\mathbf{M}_{s+1}+\frac{\alpha'}{\beta'\Delta t}\mathbf{C}_{s+1}\\
\hat{\mathbf{F}}_{s,s+1}=\mathbf{F}_{s+1}+\mathbf{M}_{s+1}\left(\frac{1}{\beta'\Delta t^2}\mathbf{X}_s+\frac{1}{\beta'\Delta t}\dot{\mathbf{X}}_s+\frac{1-2\beta'}{2\beta'}\ddot{\mathbf{X}}_s\right)\\
+\mathbf{C}_{s+1}\left(\frac{\alpha'}{\beta'\Delta t}\mathbf{X}_s+\frac{\alpha'-\beta'}{\beta'}\dot{\mathbf{X}}_s+\frac{\alpha'-2\beta'}{2\beta'}\Delta t\ddot{\mathbf{X}}_s\right)
\end{gathered}\tag{34}$$

Once the dimensionless displacement vector $\mathbf{X}$ is extracted from Eq. (33), the non-dimensional acceleration and velocity vectors can also be obtained by means of the following equations, respectively.

Table 1 Thermo-mechanical properties of the Epoxy and GPL (Heydarpour *et al*. 2019

Properties	Epoxy	GPL
Elasticity modulus (E)[GPa]	3.0	1010
Mass density (ρ) [kg/m^3]	1200	1062.5
Thermal conductivity (k) W/m	0.246	3000
Thermal expansion (α) 1/K	60×10^{-6}	5×10^{-6}
Specific heat capacity (c) J/kg.K	1110	644

$$\begin{gathered}
\ddot{\mathbf{X}}_{s+1}=\frac{1}{\beta'\Delta t^2}(\mathbf{X}_{s+1}-\mathbf{X}_s)-\frac{1}{\beta'\Delta t}\dot{\mathbf{X}}_s-\frac{1-2\beta'}{2\beta'}\ddot{\mathbf{X}}_s\\
\dot{\mathbf{X}}_{s+1}=\dot{\mathbf{X}}_s+(1-\alpha')\Delta t\ddot{\mathbf{X}}_s+\alpha'\Delta t\ddot{\mathbf{X}}_{s+1}
\end{gathered}\tag{35}$$

Utilizing the above procedure, the displacement, velocity, and acceleration vectors of the nanocomposite layer can be obtained for each time step $s\Delta t$. Since it is assumed that the layer is at rest before the loading (without initial displacement and stress) and is also at the reference temperature T_0, the initial conditions of the problem can be expressed as follows

$$u(x,0)=\theta(x,0)=\dot{u}(x,0)=\dot{\theta}(x,0)=0 \tag{36}$$

Eventually, the amount of $\mathbf{X}$ and $\dot{\mathbf{X}}$ at the first step is considered to be zero. Also, from Eq. (29), the acceleration vector for the first step is obtained zero.

7. Numerical results and discussion

In this section, the results of solving the Lord-Shulman generalized thermoelasticity problem for a viscous nano-composite layer are presented. The thermomechanical properties of the components of this type of nanocomposites are listed in Table 1. As mentioned earlier, the distribution of GPLs along the layer length is based on a power law model such that at the first of the layer, which is exposed to thermal shock is GPL rich and the other side of the layer, which is kept at room temperature, is free of any graphene. Thermal and mechanical boundary conditions related to the current analysis are demonstrated by Eqs. (16), (22). Dimensionless length of layer is considered to be $L=1$. Besides, the reference temperature $T_0=300$ K is considered. Except for Fig. 8, all the results are obtained for the middle point of the layer, $L/2$. In order to derive the response of the structure under heat load, the number of distribution points between the layers is $N_x=151$ and also each time step is equal to $\Delta t=0.001$, which are very suitable for the convergence of the response (Kiani and Eslami 2017). Also, the interfacial thermal resistance coefficient is considered as $R_k=10^{-8}$ (Yang *et al*. 2017b). The findings obtained from the Halpin-Tsai homogenization formula are very similar to the experimental results when the amplifier dimensions are in accordance, with $a_{GPL}=2.5\mu$m, $b_{GPL}=1.5\mu$m, $t_{GPL}=1.5$nm (Rafiee 2011). As a consequence, the dimensions used in this analysis are the same as in previous test (Rafiee 2011).

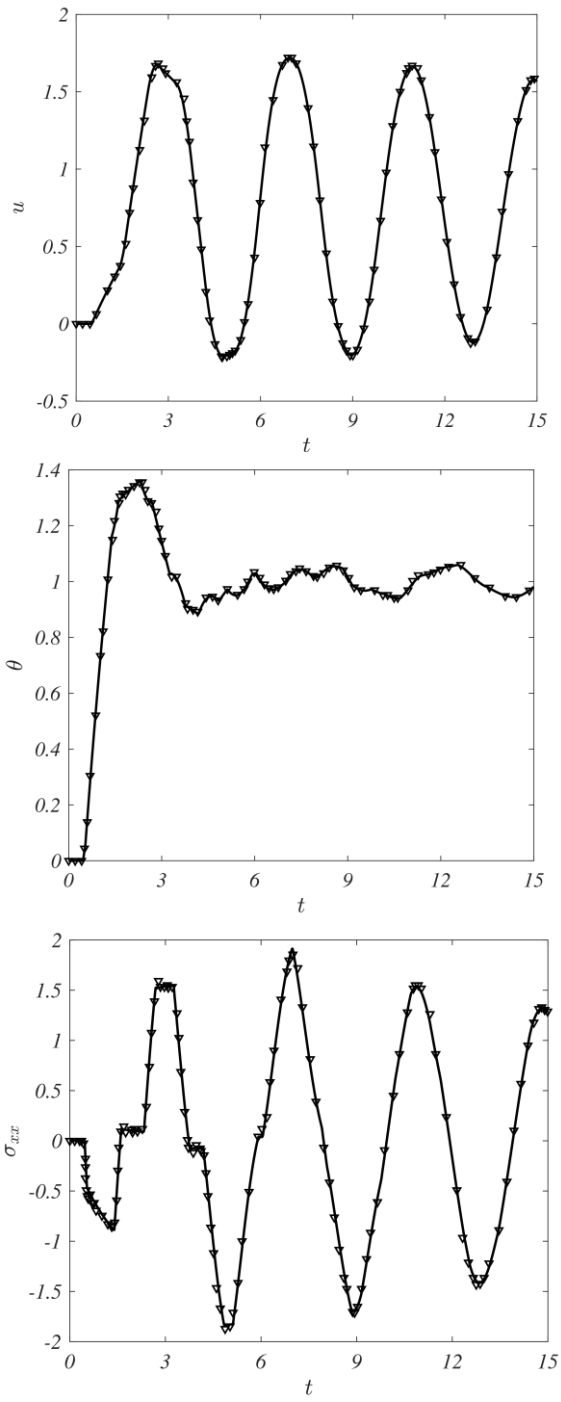

Fig. 2 The comparison of temporal evolution of displace ment (u), temperature (θ), and stress (σ_{xx}) of an isotr opic layer mid-point. (solid-line: [and Eslami 2017], tri angles: Present)

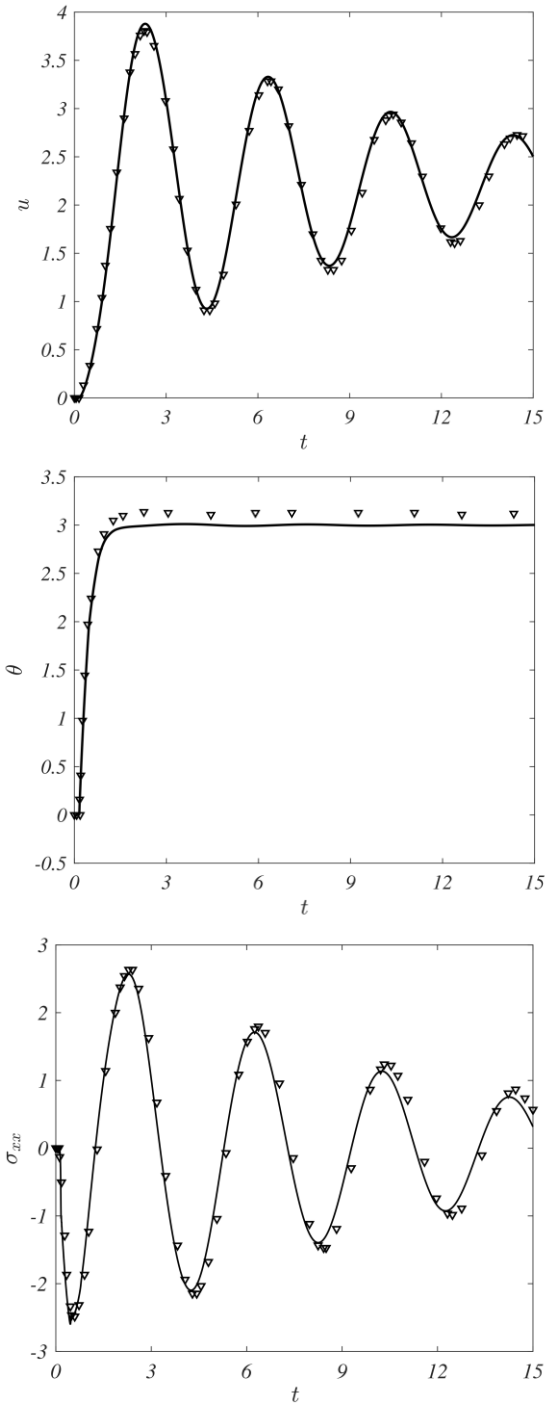

Fig. 3 The comparison of temporal evolution of displace ment (u), temperature (θ), and stress (σ_{xx}) of an isotro pic viscous layer mid-point. (solid-line: [~al.2020], trian gles: Present)

7.1 Comparison studies

As discussed before, no investigation is available on the generalized thermoelasticity response of a viscous FG-GPLRC layer. Accordingly, in order to ensure the formulation examined in this paper, comparative studies have been carried out solely for the isotropic layers.

The first comparison for the isotropic layer under thermal loading is performed with an article by Kiani and Eslami (2017). This example is illustrated in Fig. 2. This comparison is based on the thermally linear assumption. Thermal and mechanical boundary conditions are similar to the boundary conditions presented in Eqs. (16), (22). To continue the comparison process, the amount of dimension-less thermal shock is $q_i = 2$, the relaxation time is $t_0 = 1$ and the coupling coefficient is $C_T = 0.02111$ which is the coupling coefficient for the Aluminum. In this study the effect of viscosity is not applied. An excellent concurrence

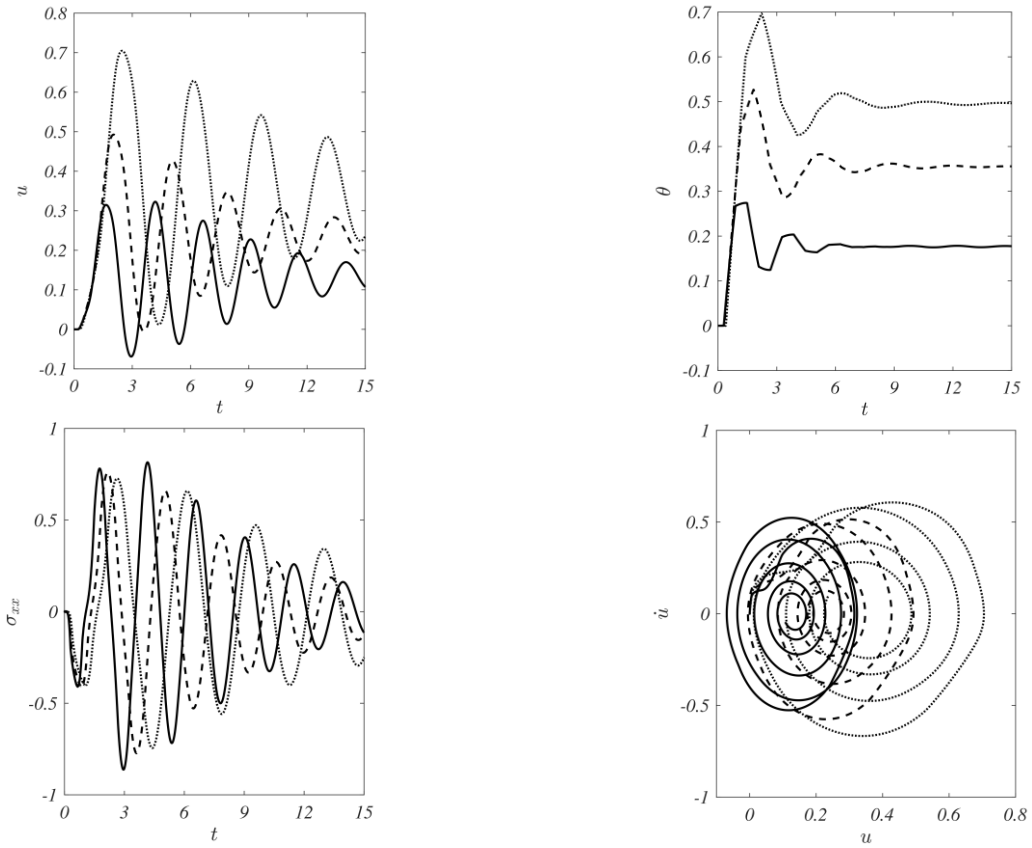

Fig. 4 The effect of power law index on the temporal evolution of displacement (u), temperatu-re (θ), and stress (σ_{xx}) associated phase-plane ($u-\dot{u}$) of FG-GPLRC layer mid-point. (solid-line: $\zeta=0$, dash-line: $\zeta=1$, dotted-line: $\zeta=5$)

Table 2 Maximum non-dimensional axial displacement and temperature in the whole time from rap-id heating considering various power-law indexes, GPL weight fractions and viscosity factors

ζ	W_{GPL}%	max	$\tau=0$	$\tau=0.05$	$\tau=0.1$
0	0.1	u	0.700	0.614	0.588
		θ	0.526	0.524	0.525
	0.5	u	0.404	0.323	0.296
		θ	0.276	0.274	0.275
	1.0	u	0.295	0.202	0.181
		θ	0.176	0.174	0.174
5	0.1	u	0.822	0.781	0.752
		θ	0.691	0.693	0.694
	0.5	u	0.741	0.704	0.678
		θ	0.692	0.670	0.698
	1.0	u	0.673	0.644	0.620
		θ	0.686	0.691	0.692

is observed between the results attained from this paper and by Kiani and Eslami (2017) for the distribution of displacement, temperature, and stress over time. It is also found that the selected values for the number of amplitude points N_x and time steps Δt performed very well in convergence and the results are quite valid.

Another comparison for the viscoelastic isotropic layer is shown in Fig. 3. This comparison is performed between the present article and a work by Oskouie *et al*. (2020). The dimensionless heat shock is assumed to be $q_i=6$, and the relaxation time is considered equal $t_0=0.1$. Furthermore, the coupling coefficient is selected $C_T=0.008$. As the layer is made of viscous material, the non-dimensional viscosity factor is chosen $\tau=0.08$. The results are indicated, as in the previous example, for longitudinal displacement, temperature and normal stress. There is a good coordination between the responses obtained from this article and those by Oskouie *et al*. (2020). The reason for the slight difference that is seen, especially for the temperature graph, is the consideration of themally nonlinear assumption in Oskouie's work.

Another comparison for the viscoelastic isotropic layer is shown in Fig. 3. This comparison is performed between the present article and a work by Oskouie *et al*. (2020). The dimensionless heat shock is assumed to be $q_i=6$, and the relaxation time is considered equal $t_0=0.1$. Furthermore, the coupling coefficient is selected $C_T=0.008$. As the layer is made of viscous material, the non-dimensional viscosity factor is chosen $\tau=0.08$. The results are indicated, as in the previous example, for longitudinal displacement, temperature and normal stress. There is a good coordination between the responses obtained from this article and those by Oskouie *et al*. (2020). The reason for the slight difference that is seen, especially for the temperature graph, is the consideration of themally nonlinear assumption in Oskouie's work.

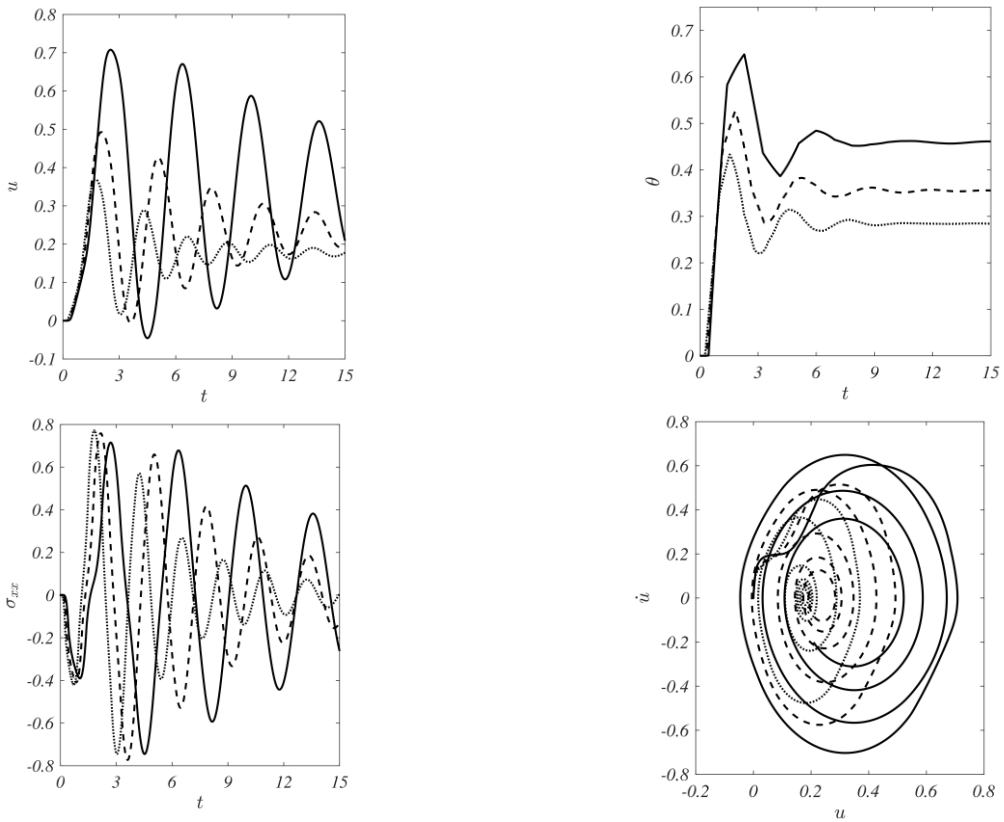

Fig. 5 The effect of GPL weight fraction on the temporal evolution of displacement (u), temperature (θ), and stress (σ_{xx}) associated phase-plane ($u-\dot{u}$) of FG-GPLRC layer mid-point. (solid-lin e: $W_{GPL}=0.1\%$, dash-line: $W_{GPL}=0.5\%$, dotted-line: $W_{GPL}=1.0\%$)

7.2 Parametric studies

In the parametric part, the parameters affecting the longitudinal displacement, temperature, stress and phase plane within the framework of Lord-Shulman theory, are investigated. In all results it is considered that the layer is subjected to dimensionless thermal shock $q_i=1$.

The first study analyzes the maximum axial displacement and temperature for various GPL weight fractions, power-law index, and viscosity factor in Table 2. In this example, the time relaxation is assumed as $t_0=1$. It is observed that the maximum deflection that occurs in temporal evolution decreases with an improvement of the viscosity factor. Also, the effect of the viscosity factor on the maximum temperature is negligible. The addition of GPLs can significantly reduce the deformation and temperatures due to increased mechanical and thermal stiffness. As mentioned before and discussed in the following results, the maximum deformation and temperature increase with an improvement of the power-law index because the amounts of total GPLs are reduced.

As the next study, Fig. 4 provides information about the influence of power law index (ζ) which determines the GPL distribution profile on the structure response. This study is performed for a nanocomposite layer with the time relaxation $t_0=1$. The weight fraction of GPL at the thermally loaded edge is $W_{GPL}=0.5\%$. Also, the viscosity factor is chosen equal $\tau=0.05$. This example is demonstrated for three amount of power law index $\zeta=0,1,5$. As mentioned earlier, when the magnitude of the power law increases, the amounts of GPLs along the layer decrease. As a result, the elastic and thermal stiffnesses of the structure changes, followed by a remarkable increase in midpoint temperature and displacement. On the other hand, by reducing the volume of GPL applied in the nano-composite, the elastic stiffness of the structure decreases, so the structure vibration frequency greatly diminishes and the damping speed of displacement, temperature and stress are also extenuated. Furthermore, it can be viewed with respect to the phase plane, that with the growth of the power law index, the maximum velocity of the midpoint occurs in bigger displacements. In addition, the structure experiences higher velocities along the time.

The effect of GPL weight fraction on the wave propagation of axial displacement, stress, and temperature and also on the related phase plane for a GPL-based nano-composite media is illustrated in Fig. 5. To implement the formulation of this example, the values of $\zeta=1$, $t_0=1$, $\tau=0.05$ are considered. These figures are prepared for three GPL weight fractions of $W_{GPL}=0.1,0.5,1\%$. Similar to the previous case, increasing the amount of GPL significantly raises the frequency of vibrations as well as the damping speed, which is attributable to the improvement in elastic stiffness caused by adding more GPL. Furthermore, with increasing the amount of GPL and subsequent increase in elastic stiffness, decrease in the amplitude of displacements is observed.

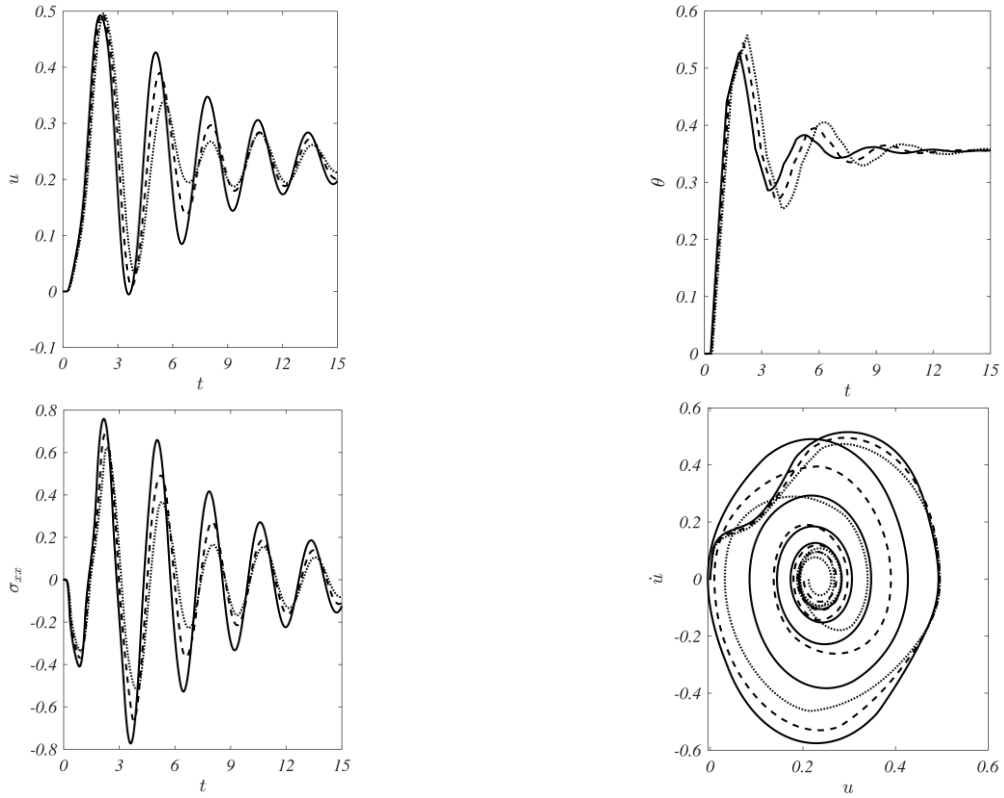

Fig. 6 The effect of relaxation time on the temporal evolution of displacement (u), temperature (θ), and stress (σ_{xx}) associated phase-plane ($u-\dot{u}$) of FG-GPLRC layer mid-point. (solid-line: $t_0 = 1.0$, dash-line: $t_0 = 1.25$, dotted-line: $t_0 = 1.5$)

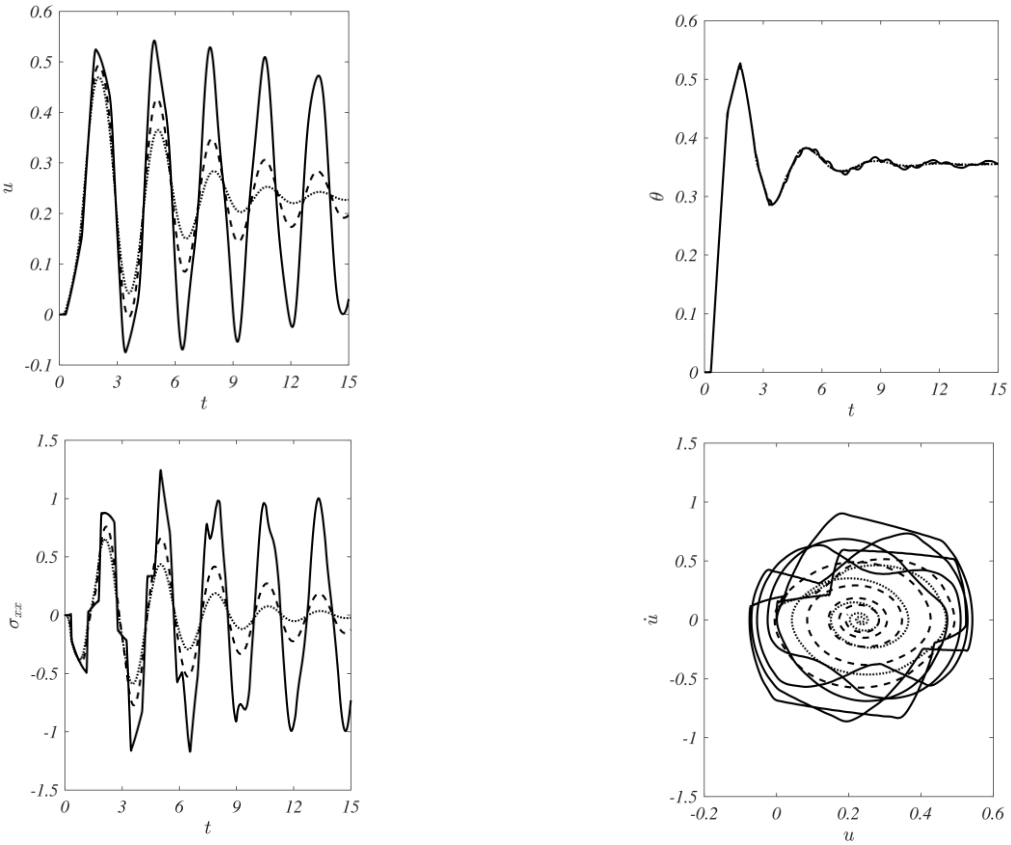

Fig. 7 The effect of viscosity factor on the temporal evolution of displacement (u), temperature (θ), and stress (σ_{xx}) associated phase-plane ($u-\dot{u}$) of layer mid-point. (solid-line: $\tau = 0.0$, dash-line: $\tau = 0.05$, dotted-line: $\tau = 0.1$)

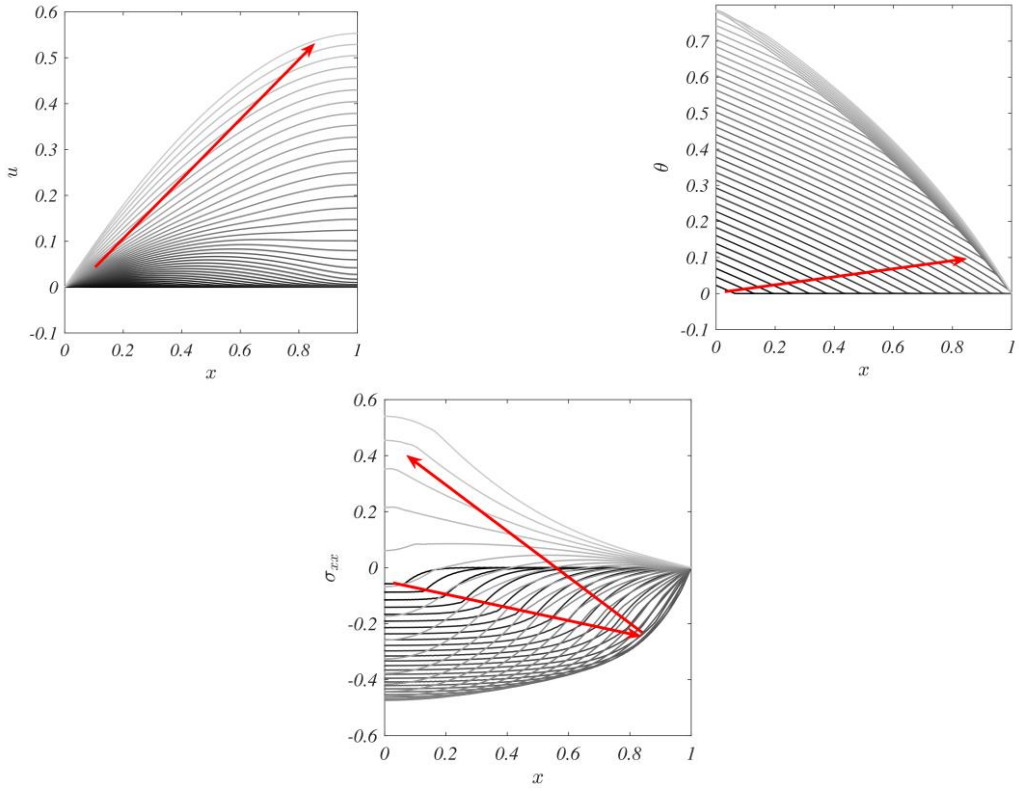

Fig. 8 propagation of displacement, temperature, and axial stress of whole layer under rapid he-ating. ($0.04 \leq t \leq 1.6$, and $t_{i+1} - t_i = 0.04$ where i indicates each line.)

Next case study indicates the time relaxation impact on the thermo-viscoelasticity response of the GPL reinforced layer in Fig. 6. Other coefficients are assumed as $\zeta = 1$, $W_{GPL} = 0.5\%$, and $\tau = 0.05$. Each subfigure of this study includes 3 line graph which deal various relaxation times $t_0 = 1, 1.25, 1.5$. When the findings are compared, it is obvious that growing the nanocomposite layer's relaxation time decreases vibration frequency. The amplitude of temperature vibrations within the system increases, while the amplitude of displacement vibrations decreases due to the interaction of thermal and elastic waves.

Another example is figured to examine the influence of viscosity factor on the temporal evolution of temperature, displacement, stress, and phase plane in Fig. 7. For the outcomes of this analysis a nanocomposite strip is assumed with $\zeta = 1$, $W_{GPL} = 0.5\%$, and $t_0 = 1$. Three amounts are selected for the viscosity factor which are $\tau = 0, 0.05, 0.1$. It can be viewed that the viscosity factor has a negligible effect on the temperature profile in time. Growing the viscosity factor, on the other hand, results in substantial damping of displacement vibrations and structural stresses.

Final result is provided in Fig. 8 to demonstrate the wave fronts movement of axial displacement, temperature, and axial stress in the whole layer. Thermo-viscoelastic parameters are defined as $\zeta = 1$, $W_{GPL} = 0.5\%$, $t_0 = 1$, $\tau = 0.05$. Each line corresponds to a specific time and represents the values shown in the vertical vector. The results are prepared for a time range of $0.04 \leq t \leq 1.6$, in which the color of the lines changes slowly from black to white over time. In other words, changes to each variable start at $t_s = 0.04$, marked in black. The lines are drawn with a time interval of $t_{i+1} - t_i = 0.04$. Until the last line (the brightest line) is related to time $t_l = 1.6$. The red arrows indicate the wave propagation direction of temperature, displacement, and stress. This example clearly demonstrates the boundary conditions used in the current problem. Since the displacement is locked at the beginning of the layer, the stress created in the structure due to the heat shock is seen as compression until the stress wave reaches the end of the strip. In that part, because the stress at the end of the structure is zero, then the stress wave is created in the form of tension and neutralizes the compressive stress that already exists in the structure until it reaches the beginning of the beam again. In that part, the stress is not zero and therefore the stress wave still moves in a tensile manner and a positive stress is created in the structure.

8. Conclusions

Wave propagation of displacement and temperature in a viscous nanocomposite media is investigated. Formulation of this research is extracted based on the generalized thermoelasticity. Homogenization techniques with second-order correlation are used to acquire the effective material properties of FG-GPLRC one dimensional domain. The Kelvin-Voigt type of viscosity is applied to derive the viscoelastic stress-strain relations. After making dimension-less, the two coupled equations derived using Lord-

Shulman theory are solved employing the GDQ and Newmark methods. Various parametric examples are illustrated to examine the material effect on the FG-GPLRC layer under the rapid heating. The findings of this article can be categorized as follows:

• For the selected functionally graded function, increase of power law index, significantly increases the temperature and displacement amplitude and converged magnitude in the structure. It also diminishes the speed of damping and the vibration frequencies.

• A greater weight fraction of GPL increases the frequency and speed of damping with a constant value of the power law index while decrease the vibration amplitudes and the static deformations.

• The amplitude of temperature vibrations and the amount of temperature fluctuations are improved as the structure's relaxation time increases. In addition, the amplitude of displacement changes and axial stress becomes smaller.

• Although the viscosity factor has no consequence on the temporal evolution of temperature, it has a serious influence on the amplitude of displacement vibrations and stresses inside the strip.

Acknowledgment

The research is partially funded by the Ministry of Science and Higher Education of the Russian Federation as part of World-class Research Center program: Advanced Digital Technologies (contract No. 075-15-2022-312 dated 20.04.2022)

References

Affdl, J.H. and Kardos, J.L. (1976), "The HalpinTsai equations: A review", *Polym. Eng. Sci.*, **16**(5), 344-352. https://doi.org/10.1002/pen.760160512.

Akbas, S.D. (2018), "Forced vibration analysis of cracked functionally graded microbeams", *Adv. Nano Res.*, **6**(1), 39-55. https://doi.org/10.12989/anr.2018.6.1.039.

Alihemmati, J., Tadi Beni, Y. and Kiani, Y. (2021), "Application of Chebyshev collocation method to unified generalized thermo-elasticity of a finite domain", *J. Therm. Stresses*, **44**(5), 547-565. https://doi.org/10.1080/01495739.2020.1867941.

Arefi, M., Bidgoli, E.M.R., Dimitri, R. and Tornabene, F. (2018), "Free vibrations of functionally graded polymer composite nanoplates reinforced with graphene nanoplatelets", *Aerosp. Sci. Technol.*, **81**, 108-117. https://doi.org/10.1016/j.ast.2018.07.036.

Arefi, M., Bidgoli, E.M.R., Dimitri, R., Bacciocchi, M. and Tornabene, F. (2019a), "Nonlocal bending analysis of curved nanobeams reinforced by graphene nanoplatelets", *Compos. B: Eng.*, **166**, 1-12. https://doi.org/10.1016/j.compositesb.2018.11.092.

Arefi, M., Bidgoli, E.M.R. and Rabczuk, T. (2019b), "Effect of various characteristics of graphene nanoplatelets on thermal buckling behavior of FGRC micro plate based on MCST", *Eur. J. Mech. A/Solids*, **77**, 103802. https://doi.org/10.1016/j.euromechsol.2019.103802.

Arefi, M., Bidgoli, E.M.R. and Rabczuk, T. (2019c), "Thermo-mechanical buckling behavior of FG GNP reinforced micro plate based on MSGT", *Thin-Walled Struct.*, **142**, 444-459. https://doi.org/10.1016/j.tws.2019.04.054.

Arefi, M., Firouzeh, S., Bidgoli, E.M.R. and Civalek, Ö. (2020), "Analysis of porous micro-plates reinforced with FG-GNPs based on Reddy plate theory", *Compos. Struct.*, **247**, 112391. https://doi.org/10.1016/j.compstruct.2020.112391.

Bagri, A., Taheri, H., Eslami, M.R. and Fariborz, S. (2006a), "Generalized coupled thermoelasticity of a layer", *J. Therm. Stresses*, **29**(4), 359-370. https://doi.org/10.1080/01495730500360492.

Bagri, A., Eslami, M.R. and Samsam-Shariat, B.A. (2006b), "Generalized coupled thermoelastic- ity of functionally graded layers", *Eng. Syst. Des. Anal.*, **42487**, 435-440. https://doi.org/10.1115/ESDA2006-95661

Chen, F., Chen, J., Duan, R., Habibi, M. and Khadimallah, M.A. (2022), "Investigation on dynamic stability and aeroelastic characteristics of composite curved pipes with any yawed angle", *Compos. Struct.*, **284**, 115195. https://doi.org/10.1016/j.compstruct.2022.115195.

Chu, K., Jia, C.C. and Li, W.S. (2012), "Effective thermal conductivity of graphene-based composites", *Appl. Phys. Lett.*, **101**(12), 121916. https://doi.org/10.1063/1.4754120.

Dong, Y., Gao, Y., Zhu, Q., Moradi, Z. and Safa, M. (2022), "TE-GDQE implementation to investigate the vibration of FG composite conical shells considering a frequency controller solid ring", *Eng. Anal. Bound. Elem.*, **138**, 5-107. https://doi.org/10.1016/j.enganabound.2022.01.017.

Ebrahimi, F. and Habibi, S. (2017), "Low-velocity impact response of laminated FG- CNT reinforced composite plates in thermal environment", *Adv. Nano Res.*, **5**(2), 69-97. https://doi.org/10.12989/anr.2017.5.2.069.

Ebrahimi, F., Habibi, M. and Safarpour, H. (2019), "On modeling of wave propagation in a thermally affected GNP-reinforced imperfect nanocomposite shell", *Eng. Comput.*, **35**, 1375-1389. https://doi.org/10.1007/s00366-018-0669-4.

Esmaeilzadeh, M., Esmaeil Golmakani, M., Kadkhodayan, M., Amoozgar, M. and Bodaghi, M. (2021), "Geometrically nonlinear thermo-mechanical analysis of graphene-reinforced moving polymer nanoplates", *Adv. Nano Res.*, **10**(2), 151-163. https://doi.org/10.12989/anr.2021.10.2.151.

Ezzat, M.A., Othman, M.I. and El-Karamany, A.S. (2002), "State space approach to two-dimensional generalized thermovisco-elasticity with one relaxation time", *J. Therm. Stresses*, **25**(3), 295-316. https://doi.org/10.1080/014957302317262323.

Gao, T., Li, C., Zhang, Y., Yang, M., Jia, D., Jin, T., Hou, Y. and Li, R. (2019), "Dispersing mechanism and tribological performance of vegetable oil-based CNT nanofluids with different surfactants", *Tribol. Int.*, **131**, 51-63. https://doi.org/10.1016/j.triboint.2018.10.025.

Gao, T., Li, C., Jia, D., Zhang, Y., Yang, M., Wang, X., Cao, H., Li, R., Ali, H.M. and Xu, X. (2020), "Surface morphology assessment of CFRP transverse grinding using CNT nanofluid minimum quantity lubrication", *J. Clean. Prod.*, **277**, 123328. https://doi.org/10.1016/j.jclepro.2020.123328.

Green, A.E. and Lindsay, K.A. (1972), "Thermoelasticity", *J. Elast.*, **2**(1), 1-7. https://doi.org/10.1007/BF00045689.

Green, A.E. and Naghdi, P.M. (1991), "A re-examination of the basic postulates of thermomechanics", *Proc. Math. Phys. Eng. Sci.*, **432**(1885), 171-194. https://doi.org/10.1098/rspa.1991.0012.

Green, A.E. and Naghdi, P.M. (1992), "On undamped heat waves in an elastic solid", *J. Therm. Stresses*, **15**(2), 253-264. https://doi.org/10.1080/01495739208946136.

Guo, X., Liu, Y. and Wang, G. (2021a), "Computer modeling for frequency performance of viscoelastic magneto-electro-elastic annular micro/nanosystem via adaptive tuned deep learning neural network optimization", *Adv. Nano Res.*, **11**(2), 203-218. https://doi.org/10.12989/anr.2021.11.2.203.

Guo, Y., Mi, H. and Habibi, M. (2021b), "Electromechanical

energy absorption, resonance frequency, and low-velocity impact analysis of the piezoelectric doubly curved system", *Mech. Syst. Signal Process.*, **157**, 107723. https://doi.org/10.1016/j.ymssp.2021.107723.

Habibi, M., Hashemabadi, D. and Safarpour, H. (2019a), "Vibration analysis of a high-speed rotating GPLRC nanostructure coupled with a piezoelectric actuator", *Eur. Phys. J. Plus*, **134**, 1-23. https://doi.org/10.1140/epjp/i2019-12742-7.

Habibi, M., Mohammadgholiha, M. and Safarpour, H. (2019b), "Wave propagation characteristics of the electrically GNP-reinforced nanocomposite cylindrical shell", *J. Braz. Soc. Mech. Sci. Eng.*, **41**, 1-15. https://doi.org/10.1007/s40430-019-1715-x.

Hajilak, Z.E., Pourghader, J., Hashemabadi, D., Bagh, F.S., Habibi, M. and Safarpour, H. (2019), "Multilayer GPLRC composite cylindrical nanoshell using modified strain gradient theory", *Mech. Based Des. Struct. Mach.*, **47**(5), 21-545. https://doi.org/10.1080/15397734.2019.1566743.

Hashemi, R., Mirzaei, M. and Adlparvar, M.R. (2021a), "On thermally induced instability of FG-CNTRC cylindrical panels", *Adv. Nano Res.*, **10**(1), 43-57. https://doi.org/10.12989/anr.2021.10.1.043.

Hashemi, H.R., Alizadeh, A.A., Oyarhossein, M.A., Shavalipour, A., Makkiabadi, M. and Habibi, M. (2021b), "Influence of imperfection on amplitude and resonance frequency of a reinforcement compositionally graded nanostructure", *Waves Random Complex Med.*, **31**(6), 1340-1366. https://doi.org/10.1080/17455030.2019.1662968.

Hetnarski, R.B. and Eslami, M.R. (2009), *Thermal Stresses: Advanced Theory and Applications*, New York, Springer. https://doi.org/10.1007/978-1-4020-9247-3.

Hetnarski, R.B. and Ignaczak, J. (1999), "Generalized thermo-elasticity", *J. Therm. Stresses*, **22**(4-5), 451-476. https://doi.org/10.1080/014957399280832.

Hetnarski, R.B. and Ignaczak, J. (2000), "Nonclassical dynamical thermoelasticity", *Int. J. Solids Struct*, **37**(1-2), 215-224. https://doi.org/10.1016/S0020-7683(99)00089-X.

Heydarpour, Y., Malekzadeh, P. and Gholipour, F. (2019), "Thermoelastic analysis of FG-GPLRC spherical shells under thermo-mechanical loadings based on Lord-Shulman theory", *Compos. B. Eng.*, **164**, 400-424. https://doi.org/10.1016/j.compositesb.2018.12.073.

Heydarpour, Y., Malekzadeh, P., Dimitri, R. and Tornabene, F. (2020), "Thermoelastic analysis of rotating multilayer FG-GPLRC truncated conical shells based on a coupled TDQM-NURBS scheme", *Compos. Struct.*, **235**, 111707. https://doi.org/10.1016/j.compstruct.2019.111707.

Hosseini, S.M. and Zhang, C. (2018), "Coupled thermoelastic analysis of an FG multilayer graphene platelets-reinforced nanocomposite cylinder using meshless GFD method: A modified micromechanical model", *Eng. Anal. Bound. Elem.*, **88**, 80-92. https://doi.org/10.1016/j.enganabound.2017.12.010.

Hosseini-Tehrani, P. and Eslami, M.R. (2000a), "Boundary element analysis of coupled thermoelasticity with relaxation times in finite domain", *AIAA J.*, **38**(3), 534-541. https://doi.org/10.2514/2.993.

Hosseini-Tehrani, P. and Eslami, M.R. (2000b), "BEM analysis of thermal and mechanical shock in a two-dimensional finite domain considering coupled thermoelasticity", *Eng. Anal. Bound. Elem.*, **24**(3), 249-257. https://doi.org/10.1016/S0955-7997(99)00063-6.

Hosseini-Tehrani, P. and Eslami, M.R. (2003), "Boundary element analysis of finite domains under thermal and mechanical shock with the Lord-Shulman theory", *J. Strain Anal. Eng. Des.*, **38**(1), 53-64. https://doi.org/10.1243/030932403762671890.

Javani, M., Kiani, Y., Shakeri, M. and Eslami, M.R. (2021), "A unified formulation for thermo- viscoelasticity of hollow sphere based on the second sound theories", *Thin-Walled Struct.*, **158**, 107167. https://doi.org/10.1016/j.tws.2020.107167.

Javani, M., Kiani, Y., Sadighi, M. and Eslami, M.R. (2019), "Nonlinear vibration behavior of rapidly heated temperature-dependent FGM shallow spherical shells", *AIAA J.*, **57**(9), 4071-4084. https://doi.org/10.2514/1.J058240.

Kanoria, M. and Mallik, S.H. (2010), "Generalized thermo-viscoelastic interaction due to periodically varying heat source with three-phase-lag effect", *Eur. J. Mech. A/Solids*, **29**(4), 695-703. https://doi.org/10.1016/j.euromechsol.2010.02.005.

Karimi Zeverdejani, P. and Kiani, Y. (2020), "Nonlinear generalized thermoelasticity of FGM finite domain based on Lord-Shulman theory", *Waves Random Complex Med.*, 1-22. https://doi.org/10.1080/17455030.2020.1788746.

Kartashov, E.M. (2014), "A generalized model of a thermal shock to viscoelastic bodies based on the Maxwell and Kelvin rheological models", *J. Eng. Phys. Thermophys.*, **87**(2), 277-288. https://doi.org/10.1007/s10891-014-1011-7.

Kiani, Y. and Eslami, M.R. (2017), "Nonlinear generalized thermoelasticity of an isotropic layer based on Lord-Shulman theory", *Eur. J. Mech. A/Solids*, **61**, 245-253. https://doi.org/10.1016/j.euromechsol.2016.10.004.

Lord, H.W. and Shulman, Y. (1967), "A generalized dynamical theory of thermoelasticity", *J. Mech. Phys. Solids*, **15**(5), 299-309. https://doi.org/10.1016/0022-5096(67)90024-5.

Mirzaei, M. (2020), "LordShulman nonlinear generalized thermo-viscoelasticity of a strip", *Int. J. Struct. Stab.*, **20**(2), 2050017. https://doi.org/10.1142/S0219455420500170.

Misra, J.C. and Samanta, S.C. (1982), "Thermal shock in a viscoelastic half-space", *J. Therm. Stresses*, **5**(3-4), 365-375. https://doi.org/10.1080/01495738208942156.

Moradi, Z., Davoudi, M., Ebrahimi, F. and Ehyaei, A.F. (2024), "Intelligent wave dispersion control of an inhomogeneous micro-shell using a proportional-derivative smart controller", *Waves Random Complex Med.*, **34**(2), 1017-1040. https://doi.org/10.1080/17455030.2021.1926572.

Nikolarakis, A.M. and Theotokoglou, E.E. (2017), "Thermal shock problem of a three-layered functionally graded zirconia/titanium alloy strip based on a unified generalized thermoelasticity theory", *J. Therm. Stresses*, **40**(5), 583-602. https://doi.org/10.1080/01495739.2016.1237860.

Oskouie, M.F., Ansari, R. and Rouhi, H. (2020), "Studying nonlinear thermomechanical wave propagation in a viscoelastic layer based upon the Lord-Shulman theory", *Mech. Adv. Mater. Struct*, **27**(10), 800-806. https://doi.org/10.1080/15376494.2018.1495793.

Othman, M.I. (2005), "Effect of rotation and relaxation time on a thermal shock problem for a half-space in generalized thermo-viscoelasticity", *Acta Mech.*, **174**(3), 129-143. https://doi.org/10.1007/s00707-004-0190-2.

Othman, M.I., Atwa, S.Y. and Farouk, R.M. (2009), "The effect of diffusion on two-dimensional problem of generalized thermo-elasticity with Green-Naghdi theory", *Intl. Comm. Heat Mass Transf.*, **36**(8), 857-864. https://doi.org/10.1016/j.icheatmasstransfer.2009.04.014.

Oyarhossein, M.A., Alizadeh, A.A., Habibi, M., Makkiabadi, M., Daman, M., Safarpour, H. and Jung, D.W. (2020), "Dynamic response of the nonlocal strain-stress gradient in laminated polymer composites microtubes", *Sci. Rep.*, **10**(1), 5616. https://doi.org/10.1038/s41598-020-61855-w.

Rafiee, M.A. (2011), "Graphene-based composite materials", Ph.D. Rensselaer Polytechnic Institute: Troy, New York, U.S.A.

Rakshit, M. and Mukhopadhyay, B. (2007), "A two dimensional thermoviscoelastic prob- lem due to instantaneous point heat source", *Math. comput. model.*, **46**(11-12), 1388-1397. https://doi.org/10.1016/j.mcm.2006.11.036.

Roychoudhuri, S.K. and Mukhopadhyay, S. (2000), "Effect of rotation and relaxation times on plane waves in generalized

thermo-visco-elasticity", *Int. J. Math. Sci.*, **23**(7), 497-505. https://doi.org/10.1155/S0161171200001356.

Safari, M., Mohammadimehr, M. and Ashrafi, H. (2021), "Free vibration of electro-magneto-thermo sandwich Timoshenko beam made of porous core and GPLRC", *Adv. Nano Res.*, **10**(2), 115-128. https://doi.org/10.12989/anr.2021.10.2.115.

Shao, Y., Zhao, Y., Gao, J. and Habibi, M. (2021), "Energy absorption of the strengthened viscoelastic multi-curved composite panel under friction force", *Arch. Civ. Mech. Eng.*, **21**(4), 141. https://doi.org/10.1007/s43452-021-00279-3.

Sharma, K. and Kumar, P. (2013), "Propagation of plane waves and fundamental solution in thermoviscoelastic medium with voids", *J. Therm. Stresses*, **36**(2), 94-111. https://doi.org/10.1080/01495739.2012.720545.

Taheri, H., Fariborz, S. and Eslami, M.R. (2004), "Thermoelasticity solution of a layer using the Green-Naghdi model", *J. Therm. Stresses*, **27**(9), 795-809. https://doi.org/10.1080/01495730490440190.

Tzou, D. (1995), "A unified field approach for heat conduction from macro-to micro-scales", *J. Heat Transf.*, **117**(1), 8-16. https://doi.org/10.1115/1.2822329.

Wang, Y.Z., Zhang, X.B. and Song, X.N. (2012), "A unified generalized thermoelasticity solution for the transient thermal shock problem", *Acta Mech.*, **223**(4), 735-743. https://doi.org/10.1007/s00707-011-0597-5.

Xu, W., Pan, G., Moradi, Z. and Shafiei, N. (2021), "Nonlinear forced vibration analysis of functionally graded non-uniform cylindrical microbeams applying the semi-analytical solution", *Compos. Struct.*, **275**, 114395. https://doi.org/10.1016/j.compstruct.2021.114395.

Yang, M., Li, C., Zhang, Y., Jia, D., Zhang, X., Hou, Y., Li, R. and Wang, J. (2017a), "Maximum undeformed equivalent chip thickness for ductile-brittle transition of zirconia ceramics under different lubrication conditions", *Int. J. Mach. Tools Manuf*, **122**, 55-65. https://doi.org/10.1016/j.ijmachtools.2017.06.003.

Yang, B., Yang, J. and Kitipornchai, S. (2017b), "Thermoelastic analysis of functionally graded graphene reinforced rectangular plates based on 3D elasticity", *Meccanica*, **52**(10), 2275-2292. https://doi.org/10.1007/s11012-016-0579-8.

Yang, M., Li, C., Zhang, Y., Jia, D., Li, R., Hou, Y., Cao, H. and Wang, J. (2019), "Predictive model for minimum chip thickness and size effect in single diamond grain grinding of zirconia ceramics under different lubricating conditions", *Ceram. Int.*, **45**(12), 14908-14920. https://doi.org/10.1016/j.ceramint.2019.04.226.

Yang, M., Li, C., Luo, L., Li, R. and Long, Y. (2021), "Predictive model of convective heat transfer coefficient in bone micro-grinding using nanofluid aerosol cooling", *Int. Commun. Heat Mass Transf.*, **125**, 105317. https://doi.org/10.1016/j.icheatmasstransfer.2021.105317.

Youssef, H.M. (2006), "Two-dimensional generalized thermo-elasticity problem for a half-space subjected to ramp-type heating", *Eur. J. Mech. A/Solids*, **25**(5), 745-763. https://doi.org/10.1016/j.euromechsol.2005.11.005.

Youssef, H.M. and Alghamdi, N.A. (2020), "Modeling of one-dimensional thermoelastic dual- phase-lag skin tissue subjected to different types of thermal loading", *Sci. Rep.*, **10**(1), 1-12. https://doi.org/10.1038/s41598-020-60342-6.

Youssef, H.M. and Al-Lehaibi, E.A. (2007), "State-space approach of two-temperature generalized thermoelasticity of one-dimensional problem", *Int. J. Solids Struct*, **44**(5), 1550-1562. https://doi.org/10.1016/j.ijsolstr.2006.06.035.

Youssef, H.M. and El-Bary, A.A. (2014), "Thermoelastic material response due to laser pulse heat- ing in context of four theorems of thermoelasticity", *J. Therm. Stresses*, **37**(12), 1379-1389. https://doi.org/10.1080/01495739.2014.937233.

Yu, Y.J., Hu, W. and Tian, X.G. (2014), "A novel generalized thermoelasticity model based on memory-dependent derivative", *Int. J. Eng. Sci.*, **81**, 123-134. https://doi.org/10.1016/j.ijengsci.2014.04.014.

Zad, S.H., Komeili, A., Eslami, M.R. and Fariborz, S. (2012), "Classical and generalized coupled thermoelasticity analysis in one-dimensional layered media", *Arch. Appl. Mech.*, **82**(2), 267-282. https://doi.org/10.1007/s00419-011-0555-7.

Zhang, Y., Li, C., Jia, D., Zhang, D. and Zhang, X. (2015), "Experimental evaluation of the lubrication performance of MoS2/CNT nanofluid for minimal quantity lubrication in Ni-based alloy grinding", *Int. J. Mach. Tools Manuf*, **99**, 19-33. https://doi.org/10.1016/j.ijmachtools.2015.09.003.

Zheng, Q.S. and Du, D.X. (2001), "An explicit and universally applicable estimate for the effective properties of multiphase composites which accounts for inclusion distribution", *J. Mech. Phys. Solids*, **49**(11), 2765-2788. https://doi.org/10.1016/S0022-5096(01)00078-3

AT